

(iii) The region $x > 0$ with no loss of heat from the surface $x = 0$. The initial temperature $V(1 - e^{-ax})$, and the rate of heat production $H_0 = A_0 e^{-ax}$.

The exponential form of initial temperature is chosen because the results are easy to calculate, $a = 0.56$ leads to the surface gradient of 2°C per cm used by Cook.⁽¹⁾

The surface temperature is found to be

$$\frac{A_0}{K(\beta^2 - \alpha^2)\beta} \{ \beta - \alpha \operatorname{erf} \beta \sqrt{(\kappa t)} - \beta \exp [-\kappa(\beta^2 - \alpha^2)t] \operatorname{erfc} \alpha \sqrt{(\kappa t)} \} + V - V \exp [-\kappa(\beta^2 - \alpha^2)t] \operatorname{erfc} a \sqrt{(\kappa t)} \quad (7)$$

where β is defined in equation (4). As $t \rightarrow \infty$ the surface temperature tends to

$$V + \frac{A_0}{K\beta(\beta + \alpha)} \quad (8)$$

This corresponds to the problem of Cook⁽¹⁾ in which all the quantities are known numerically so that quantitative comparison is possible. Taking the values of his Fig. 4, namely, $K = \kappa = 0.005$, $\alpha = 1.5$, $A_0 = 0.184$, assuming $V = 3.6^\circ \text{C}$ (the excess of blood heat above initial skin temperature), and that the final skin temperature is 11°C above its initial value, gives $\beta = 1.6$, which, with $c' = 1$, $K = 0.005$ in equation (4), corresponds to a blood supply of

$0.013 \text{ g per c.c. per sec}$. Curve I of the figure gives the calculated surface temperature for this case with $a = 0.56$, and Curve II the corresponding case with occlusion, $m = 0$. The dotted Curves III and IV are the corresponding observed results from Cook's Fig. 4. The fit is by no means perfect but it gives a reasonable representation of the results and it could have been improved by changing the assumed values of A_0 , α , and K .

I am indebted to Dr. Cook for pointing out that the rate of supply of blood found above, namely $0.013 \text{ g per c.c. per sec}$, is about six times the normal rate, and that this ratio seems reasonable in view of the vaso-dilatation on heating. It may also be remarked that, in the absence of other sources of heat, supply of blood at the normal rate of about $0.0022 \text{ g per c.c. per sec}$ leads to surface temperature gradients of the right order of magnitude: for example, if the surface is maintained at 3.6°C below blood heat, the steady temperature gradient at the surface will be $2.4^\circ \text{C per cm}$.

Finally it may be mentioned that the same considerations have been found useful in a study (unpublished) of the heating of the retina of the eye by infra-red radiation.

REFERENCES

- (1) COOK, H. F. *Brit. J. Appl. Phys.*, **3**, p. 1 (1952).
- (2) MENDELSSOHN, K., and ROSSITER, R. J. *Quart. J. of Exp. Physiol.*, **32**, p. 301 (1944).

The saturation curve at high ionization intensity

By J. W. BOAG, B.Sc., F.Inst.P., and T. WILSON, B.Sc.(Eng.),* Radiotherapeutic Research Unit, Hammersmith Hospital, London

[Paper received 30 January, 1952]

In this paper the form of the saturation curve is investigated theoretically and experimentally. It is shown that saturation curves taken under different conditions on a parallel plate ionization chamber are transformed into a single general curve when plotted in terms of a dimensionless product of the several variables. The experimental work utilized an ionization chamber with thin foil electrodes. A coin-shaped region between the foils was ionized by a beam of fast electrons. Dose rates up to $100\,000 \text{ e.s.u./cm}^3 \times \text{sec}$ could be attained. It is shown that very high ionization intensities can be measured in a parallel plate chamber, provided the spacing of the plates is small.

In a previous paper⁽¹⁾ formulae were developed for the proportion of ions which can be collected in a parallel-plate ionization chamber when the ionization occurs in instantaneous pulses. The problem of the ionization current flowing through a gas subjected to a continuous high radiation intensity presents greater mathematical difficulty. Although J. J. Thomson set up the general differential equation for the transport of ions between parallel plates as long ago as 1900, explicit solutions of this equation have been obtained in only a small number of special cases.⁽²⁾ The equation has been attacked by various approximate methods, notably by Mie⁽³⁾ and Seeliger.⁽⁴⁾ Seemann⁽⁵⁾ determined experimentally the saturation curve between plane parallel electrodes in air at normal atmospheric pressure, and found good agreement with Mie's numerical solution of Thomson's equation. The ionization intensity in this work was of the order of $1 \text{ e.s.u./c.c.} \times \text{min}$ and the electrode spacing varied from 1 to 5 cm.

Mie had shown that saturation curves taken under different experimental conditions should be capable of transformation

to a standard form by taking as ordinate the collection efficiency (which we shall denote by f), that is, the ratio of measured ionization current to theoretical saturation current, i/i_m , and as abscissa another dimensionless parameter, V/Ri_m ,

where $V =$ collecting voltage;

$i_m =$ saturation current;

$R =$ apparent resistance of the ionized gas at very low collecting voltage.

Seemann confirmed experimentally that a transformation of this kind was possible, but he did not determine R directly, as his apparatus was not suitable for this purpose. He merely brought the different saturation curves into coincidence at an arbitrary point near the knee of the curve (the point $f = 0.6$) and showed that, when this was done, the portions above and below the arbitrary matching point agreed extremely well. It is not easy to measure R accurately from the gradient at the origin, since curvature persists down to very low collecting voltages. Moreover, the quantity R is not usually of direct interest, nor is it of use in designing an ionization chamber for a given ionization intensity. Mie's parameter is not, therefore, the most suitable one for the abscissa of a general saturation curve.

* Now at the British Electricity Authority Research Laboratory, Leatherhead.

Table 1. Dimensional analysis

Fundamental units: Length (L), Time (T), Charge (Q)		
Name of quantity	Symbol	Dimensional formula
Collecting voltage	V	QL^{-1}
Electrode spacing	d	L
Ionization intensity	q	$QL^{-3}T^{-1}$
Recombination coefficient	α/e	$Q^{-1}L^3T^{-1}$
Ionic mobilities	k_1, k_2	$Q^{-1}L^3T^{-1}$
Ionization current density	i	$QL^{-2}T^{-1}$

The experimental variables which influence the saturation curve between plane parallel electrodes in a uniformly ionized gas, are listed in Table 1. These are all the independent quantities which enter into the differential equation governing the phenomena. Other variables, such as the field strength X at distance x from the positive plate, may also appear in the differential equation, but a subsidiary equation such as

$$V = \int_0^d X dx$$

permits each dependent variable to be eliminated from the final solution, at least in principle. The saturation curve is, of course, influenced by the type of gas used and by its temperature and pressure. These variables do not appear explicitly in Table 1 because we assume that they influence only the recombination coefficient α and the mobilities of the positive and negative ions, k_1 and k_2 . We assume:

(1) That recombination occurs at the rate $\alpha n_1 n_2$ ion pairs per cm^3 per sec where n_1, n_2 are the numbers of ions of either sign present per cm^3 , and α is a constant characteristic of the gas. This expression may equally well be written in the form $-(\alpha/e)\rho_1\rho_2$ e.s.u. of charge destroyed per cm^3 per sec where the ρ 's represent units of charge per cm^3 and e is the electronic charge.

(2) That the drift velocity of the positive ion, when in an electric field of strength X , is $k_1 X$ cm/sec in the direction of the field while that of the negative ion is $k_2 X$ in the opposite direction, k_1 and k_2 being constants.

The dimensional formulae of the several variables, in terms of the units chosen as fundamental, namely, length, time, and charge, are given in Table 1. The most general form of the product of powers of the variables is

$$(V)^\beta (d)^\gamma (q)^\delta (\alpha/e)^\epsilon (k_1)^\lambda (k_2)^\mu (i)^\nu$$

Substituting the dimensional formula for each of the variables into this expression and equating the indices of the three fundamental units to zero, we have the following three equations between the seven variables:⁽⁶⁾

$$\left. \begin{aligned} \beta + \delta - (\kappa + \lambda + \mu) + \nu &= 0 \\ -\beta + \gamma - 3\delta + 3(\kappa + \lambda + \mu) - 2\nu &= 0 \\ -\delta - (\kappa + \lambda + \mu) - \nu &= 0 \end{aligned} \right\} \quad (1)$$

After solving the equations (1) for γ, δ, λ , in terms of the other indices, we obtain for the general dimensionless product

$$\left(\frac{V\sqrt{k_1}}{d^2\sqrt{q}} \right)^\beta \left(\frac{\alpha}{ek_1} \right)^\epsilon \left(\frac{k_2}{k_1} \right)^\mu \left(\frac{i}{qd} \right)^\nu \quad (2)$$

Since the combination of variables within each bracket is raised to an arbitrary power, each such combination must form a subsidiary dimensionless product. The general solution of the problem may then be written

$$\frac{i}{qd} = \phi \left[\frac{k_1}{k_2}, \frac{\alpha}{ek_1}, \frac{d^2\sqrt{q}}{V\sqrt{k_1}} \right] \quad (3)$$

where ϕ is an unknown function of the three dimensionless

arguments. The l.h.s. of this equation is the ratio of actual current density to saturation current density, i.e. it is the collection efficiency, f . Moreover, two of the arguments of the function ϕ involve only the mobilities, the recombination coefficient and the electronic charge. For a given gas under standard conditions all these are constant. We may, therefore, conclude that under these circumstances

$$f = \phi \left(\frac{d^2\sqrt{q}}{V} \right) \quad (4)$$

where ϕ is to be read simply as an unknown function, whose form, however, can be determined experimentally for a particular gas under standard conditions of temperature and pressure.

EXPERIMENTAL MEASUREMENTS

The ionization chambers used in this work have already been described.⁽⁷⁾ The saturation curves illustrated below were taken in a 1.2 MeV electron beam emerging from a thin aluminium window at the end of the accelerating tube of a Van de Graaff generator. The beam entering the ionization chamber was defined by a circular hole in a 3/16 in thick aluminium "stop" placed immediately above the upper aluminium foil of 0.001 in thickness which formed the chamber wall. The beam diameter was in some cases 1 cm and in others 0.7 cm. Even with the larger beam, the radial variation in ionization intensity in the chamber did not exceed 5%, so the experimental arrangement permitted a well-defined coin-shaped region between the parallel foils to be irradiated to a high and fairly uniform ionization intensity. One of the ionization chambers used (Chamber B, Fig. 1, in the paper by Boag, Pilling and Wilson⁽⁷⁾) had provision for varying the spacing of the foils, from a fraction of a millimetre up to several millimetres. In the experiments described below the two outer foils were adjusted to be at equal distances from the central foil, so that the characteristics of the two gaps from which the total current was collected were always identical.

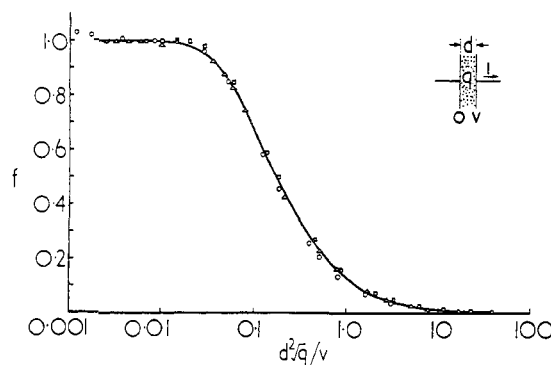


Fig. 1. General saturation curve in air at 764 mm and 17.1°C for plane parallel geometry. Ionization intensity was constant while the plate spacing was varied

$q = 1\,000$ e.s.u./c.c. \times sec.
 \circ $d = 0.0625$ cm. \triangle $d = 0.126$ cm.
 \square $d = 0.253$ cm.

In the first series of measurements the ionization intensity was set to give 1 000 e.s.u./c.c. \times sec in air at normal pressure and room temperature and saturation curves were taken for electrode spacings of 0.0625 cm, 0.125 cm and 0.25 cm. The collection efficiency in these measurements is plotted in Fig. 1 to a base of $d^2\sqrt{q}/V$, and it can be seen that (within the experimental error) the points for all three electrode spacings

lie on a single curve. The full line is based on an approximate theory which we shall discuss below.

In the second series of measurements the electrode spacing was held constant at 0.126 cm and the ionization intensity was set at 1890 e.s.u./c.c. × sec, 18 800 e.s.u./c.c. × sec and 118 000 e.s.u./c.c. × sec, successively. For each intensity a complete saturation curve was taken, and the collection efficiency for each measured point is plotted against $d^2\sqrt{q}/V$ in Fig. 2. As before, the points for all three intensities lie on a single curve, and as the full line is identical with that in Fig. 1, it can be seen that within the limits quoted—namely 0.0625 cm to 0.25 cm and 1 000 e.s.u./c.c. × sec up to 118 000 e.s.u./c.c. × sec—the collection efficiency f is indeed a function of $d^2\sqrt{q}/V$ only.

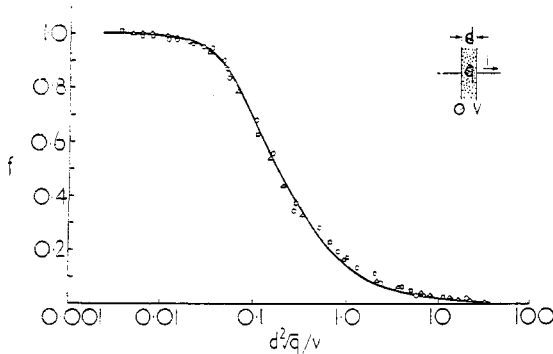


Fig. 2. General saturation curve in air at 764 mm and 17.1°C for plane parallel geometry. Spacing of plates was held constant while the ionization intensity was varied

$d = 0.126$ cm.
 ○ $q = 118\ 000$ e.s.u./c.c. × sec.
 △ $q = 18\ 800$ e.s.u./c.c. × sec.
 □ $q = 1\ 890$ e.s.u./c.c. × sec.

The curves in Figs. 1 and 2 were all taken on the same day, so that atmospheric conditions were constant. Curves taken on different days over a period of months did not always agree with one another quite so closely, but the divergences were principally at the low voltage end of the curve. As a guide to the voltage required for saturation the general curve has proved entirely satisfactory. It is proposed to investigate the effect of air pressure and temperature, but this has not yet been done.

APPROXIMATE THEORIES

By ignoring space charge, it is possible to obtain an approximate solution of Thomson's equation which should be valid in the near-saturation region. Mie's numerical solution (reference (3), Fig. 3) shows that for 90% collection efficiency

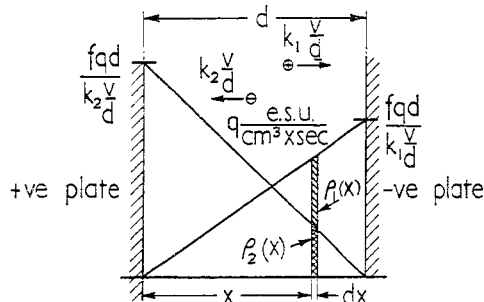


Fig. 3. Distribution of charge density in the air gap under near-saturation conditions

in air at atmospheric pressure and room temperature the field strength varies only about ± 20% from its mean value. At higher collection efficiency the variation will be less. The assumption of constant field strength between the plates may be introduced into the equations in several ways, and these lead to slightly different solutions. Thus, Townsend⁽⁸⁾ assumes that the ions of either sign move with constant velocities, $k_1(V/d)$ and $k_2(V/d)$, in the field between the electrodes. The steady state is then determined by the equations (in our notation)

$$q = \frac{\alpha}{e} \rho_1 \rho_2 + \frac{d}{dx} (\rho_1 u_1) \tag{5}$$

$$i = \rho_1 u_1 + \rho_2 u_2 \tag{6}$$

where ρ_1, ρ_2 = charge densities of positive and negative ions respectively;
 u_1, u_2 = velocities of positive and negative ions respectively;
 i = ionization current density.

The solution of these equations for u_1, u_2 constant, can be shown to be⁽⁸⁾

$$\sqrt{\left(\frac{4qu_1u_2}{(\alpha/e)i^2} - 1\right)} \tan \left[\frac{\alpha}{e} \frac{di}{4u_1u_2} \sqrt{\left(\frac{4qu_1u_2}{(\alpha/e)i^2} - 1\right)} \right] = 1 \tag{7}$$

Now putting $u_1 = k_1V/d$ $i = fqd$
 $u_2 = k_2(V/d)$

$$\xi = \sqrt{\left(\frac{\alpha}{ek_1k_2}\right) \frac{d^2\sqrt{q}}{V}} = m \frac{d^2\sqrt{q}}{V}$$

say, where m is a constant, we obtain

$$\sqrt{\left(\frac{4}{f^2\xi^2} - 1\right)} \tan \left[\frac{f\xi^2}{4} \sqrt{\left(\frac{4}{f^2\xi^2} - 1\right)} \right] \tag{8}$$

We cannot express f in terms of ξ explicitly, but the solution can be put into the parametric form

$$\left. \begin{aligned} f &= \frac{\omega}{(1 + \omega^2) \tan^{-1} \omega} \\ \xi &= 2\sqrt{(1 + \omega^2) \tan^{-1} \omega} \end{aligned} \right\} \tag{9}$$

where ω is a variable parameter, $0 < \omega < \infty$.

An alternative approximation is obtained by assuming that the positive ion density between the electrodes rises linearly from zero at the positive plate to a maximum at the negative plate, while the negative ion density varies linearly in the opposite direction. If the field were truly uniform and no recombination occurred, this model, which is illustrated in Fig. 3, would be correct. Close to the negative plate the current i is carried entirely by the positive ions whose density there is $\rho_{1\max}$, and whose velocity we take as $k_1(V/d)$. Then

$$\left. \begin{aligned} \rho_{1\max} &= \frac{i}{k_1(V/d)} = \frac{fqd^2}{k_1V} \\ \rho_{2\max} &= \frac{i}{k_2(V/d)} = \frac{fqd^2}{k_2V} \end{aligned} \right\} \tag{10}$$

The densities of positive and negative ions at any distance x from the positive plate are then

$$\left. \begin{aligned} \rho_1(x) &= \left(1 - \frac{x}{d}\right) \frac{fqd^2}{k_1V} \\ \rho_2(x) &= \frac{x}{d} \frac{fqd^2}{k_2V} \end{aligned} \right\} \tag{11}$$

and hence the average rate of recombination throughout the space is

$$\mathcal{R} = \frac{1}{d} \int_0^d \alpha \rho_1(x) \rho_2(x) dx = \frac{\alpha}{e} \frac{f^2 q^2 d^4}{6 k_1 k_2 V^2} \quad (12)$$

Now the fraction of the total charge liberated per unit volume which is destroyed by recombination is $(1 - f)$. Therefore $\mathcal{R} = (1 - f)q$. Hence

$$f = 1 - \frac{\mathcal{R}}{q} = 1 - \frac{f^2}{6} \frac{\alpha}{e k_1 k_2} \frac{d^4 q}{V^2} = 1 - \frac{1}{6} f^2 \xi^2 \quad (13)$$

where $\xi = m(d^2 \sqrt{q/V})$ as before.

This is a quadratic equation for f whose only positive root is

$$f = 2/[1 + \sqrt{(1 + \frac{1}{3} \xi^2)}] \quad (14)$$

If we calculate pairs of values of f and ξ from equation (9), and for comparison determine from equation (14) the value of f for each of these values of ξ , we find that the two equations (9) and (14) are almost entirely equivalent. This comparison is given in Table 2.

Table 2. Comparison of the values of f determined from equations (9) and (14)

	$\omega = 0.1$	0.2	0.4	0.8	1.0	2.0	4.0
Eqn. (9) $\left\{ \begin{array}{l} \frac{\alpha}{e} \\ f \end{array} \right.$	0.1994 0.9930	0.4026 0.9742	0.8196 0.9062	1.728 0.7230	2.221 0.6366	4.951 0.3613	10.933 0.1775
Eqn. (14) f	0.9934	0.9743	0.9079	0.7328	0.6512	0.3873	0.2004

We can then confine our attention to the simpler expression for f which is provided by equation (14), and can test this formula against the experimental results by regarding m as an empirical constant. The full line in Figs. 1 and 2 represents equation (14) with m put equal to 19.4. It is surprising that this formula fits the observations not only in the near-saturation region, for which the approximation was set up, but also over most of the curve.

The values of the recombination coefficient and of the ionic mobilities reported in the literature are by no means all concordant. Thomson surveyed the data up to 1927 in his book.⁽²⁾ For air at atmospheric pressure and 0° C the smallest of the several values of α/e reported is 3 200 (reference (2), p. 40). According to Erikson^(9, 10) α/e varies inversely as the 7/3 power of the absolute temperature. At 20° C one should, therefore, have $\alpha/e = 2 730$. Widely different values have been reported by different observers for k_1, k_2 in air. Thomson's survey recommends

$$\left\{ \begin{array}{l} k_1 = 1.36 \text{ cm/sec per volt/cm} \\ k_2 = 2.1 \text{ cm/sec per volt/cm} \end{array} \right.$$

as the most probable values. However, Erikson⁽¹¹⁾ found that the positive ion, when freshly formed, had the same mobility as the normal negative ion. Substituting $\alpha/e = 2 730$, $k_1 = k_2 = 2.1$ in the expression for m we find

$$m = \sqrt{(\alpha/e k_1 k_2)} = \sqrt{(2 730 \cdot 2.1 \times 2.1)} = 24.9 \quad (15)$$

Although we have selected from the reported values of the constants those which would tend to make m as small as possible, the figure which results is considerably higher than the empirical value of 19.4. We conclude that, in our experiments, α/e was smaller than normal or $k_1 k_2$ larger. The most likely source of the discrepancy is the mobility of the negative ion. The latter is usually formed by the attachment of a free electron to a molecule, although bombardment by fast electrons does lead, in some cases, to the direct splitting of a diatomic molecule into positive and negative ions.⁽¹²⁾ With the short inter-electrode spacings and high field strengths used in our experiments, some of the electrons

may cross the gap without attachment, thus increasing the apparent value of k_2 . The extent to which this may happen is examined in the next section.

ATTACHMENT OF ELECTRONS TO MOLECULES

Only a small fraction, say $1/n$, of all collisions between free electrons and molecules result in the formation of a negative ion by electron capture. Thomson has shown (reference (2), p. 137) that the probability of an electron drifting a distance d in a uniform field of strength X without becoming attached to a molecule is then

$$P(d) = e^{-vd/n\lambda kX} = e^{-\psi}, \text{ say,}$$

where v is the velocity of agitation, λ is the mean free path, and k is the mobility of the electron in the gas under the given physical conditions. If electrons are liberated uniformly in the space between two plane electrodes at a distance d apart, then the proportion crossing unattached will be

$$P'(d) = \frac{1}{d} \int_0^d P(x) dx = (1 - e^{-\psi})/\psi \quad (16)$$

Data on the quantities n, v, λ , and on the drift velocity kX have been collected and published by Healey and Reed.⁽¹³⁾ For air their values are based on the experiments of Townsend and Tizard⁽¹⁴⁾ and of Bailey.⁽¹⁵⁾ The quantities are all functions of the ratio of field strength to gas pressure. For air at 1 atmosphere and a field strength of 2 kV/cm, the values obtained by interpolation in Healey and Reed's tables are:

$$n = 2.9 \times 10^6, v = 6 \times 10^7 \text{ cm/sec}, \lambda = 4.2 \times 10^{-5} \text{ cm and } kX = 2.1 \times 10^6 \text{ cm/sec.}$$

Hence

$$\psi = \frac{vd}{n\lambda kX} = \frac{6 \times 10^7 \times d}{2.9 \times 10^6 \times 4.2 \times 10^{-5} \times 2.1 \times 10^6} = 0.234 d = 0.0234 \text{ for } d = 0.1 \text{ cm}$$

In this case $P'(d) = (1 - e^{-\psi})/\psi = 0.985$ and so only 1.5% of the electrons would form ions in crossing a 1 mm gap with 200 V across it. It must be noted, however, that the value of n which should be used is very uncertain. Thus Loeb^(16, 17) found $n = 0.7-6.4 \times 10^4$ in air at atmospheric pressure for small field strengths. Moreover, Healey and Reed's value refers to dry air, and a small amount of moisture may increase the probability of attachment (reference (2), p. 155). If the true value of n for our experimental conditions were 1/10 of the value used above we should have $P' = 0.893$; if it were 1/100, $P' = 0.386$. It seems that for a 1 mm gap and a field of 2 kV/cm, which is typical of the field strength required to produce saturation in many of our experiments, a considerable proportion of the electrons liberated in the gap will reach the positive plate without having formed ions.

The approximate formulae derived in an earlier section to represent the saturation curve were based on the assumption that the mobilities of the positive and negative ions were independent of the field strength. Free electrons do not show a constant mobility (reference (2), p. 146). Moreover, we had assumed that the field in the near-saturation region would be almost uniform across the gap. If a considerable proportion of the negative charge carriers are electrons, there will be a residual positive space charge and the field at the negative plate will always be higher, and often much higher, than at the positive plate. It appears that, under these conditions, a different approach must be made. In some gases,

such as argon and hydrogen, electron attachment does not occur, and, in the absence of impurities, the current should be carried by positive ions and electrons only. It is of interest to consider this case, if only because conduction in air must lie somewhere between this extreme and the other, for which we have already obtained an approximate solution.

CONDUCTION BY POSITIVE IONS AND ELECTRONS

The drift velocity of electrons in an electric field is about one thousand times that of positive ions, and in the near-saturation region the electronic space charge is therefore negligible compared with that due to the positive ions. Instead of assuming constant field strength across the gap, we can determine the spatial variation of the field for the case in which no recombination occurs and assume that this field distribution still holds in the near-saturation region.

Let X be the field at distance x from the positive plate, and ρ_1, ρ_2 the charge densities of the positive ions and electrons, respectively, at that plane.

Then

$$\frac{dX}{dx} = 4\pi(\rho_1 - \rho_2) \tag{17}$$

$$\frac{d}{dx}(k_1 X \rho_1) = q \tag{18}$$

$$\frac{d}{dx}(k_2 X \rho_2) = -q \tag{19}$$

Combining these equations and eliminating ρ_1, ρ_2 we obtain

$$\frac{d^2 X^2}{dx^2} = 8\pi q \left(\frac{k_1 + k_2}{k_1 k_2} \right) = \theta \text{ (say)} \tag{20}$$

where θ is independent of x . Now the positive ion density in the vicinity of the positive plate is zero, and if we assume that the electron space charge, even at the positive plate, is negligible, then $dX/dx = 0$ for $x = 0$ and the solution of equation (20) is

$$X^2 = X_0^2 + (\theta/2)x^2 \tag{21}$$

where X_0 is the field at the positive plate. We may write this as

$$\left(\frac{X}{X_0} \right)^2 = 1 + \zeta^2 \left(\frac{x}{d} \right)^2 \tag{22}$$

with
$$\zeta = \sqrt{\left[\frac{4\pi(k_1 + k_2)}{k_1 k_2} \right]} \frac{d\sqrt{q}}{X_0}$$

Now

$$\begin{aligned} V = \int_0^d X dx &= X_0 d \int_0^1 \left(\frac{X}{X_0} \right) d \left(\frac{x}{d} \right) = X_0 d \int_0^1 \sqrt{1 + \zeta^2 u^2} du \\ &= \frac{X_0 d}{2} \left\{ \sqrt{1 + \zeta^2} + \frac{1}{\zeta} \log \left[\zeta + \sqrt{1 + \zeta^2} \right] \right\} \end{aligned}$$

Hence

$$\sqrt{\left[\frac{k_1 k_2}{4\pi(k_1 + k_2)} \right]} \frac{V}{d^2 \sqrt{q}} = \frac{1}{2} \sqrt{\left[\frac{k_1 k_2}{4\pi(k_1 + k_2)} \right]} \frac{X_0}{d \sqrt{q}} \left\{ \sqrt{1 + \zeta^2} + \frac{1}{\zeta} \log \left[\zeta + \sqrt{1 + \zeta^2} \right] \right\}$$

or
$$\frac{1}{\xi^2} = \frac{1}{2\xi^2} \left\{ \sqrt{1 + \zeta^2} + \frac{1}{\zeta} \log \left[\zeta + \sqrt{1 + \zeta^2} \right] \right\} \tag{23}$$

where ξ' is a dimensionless variable containing $d^2 \sqrt{q}/V$ as a factor. Equation (23) gives the value of X_0 corresponding to given values of $d, q,$ and $V,$ the mobilities k_1 and k_2 being

supposed known. Knowing $X_0,$ the field distribution between the plates is then fully determined by equation (22). The curves in Fig. 4 illustrate the shape of this distribution, for several values of ξ' .

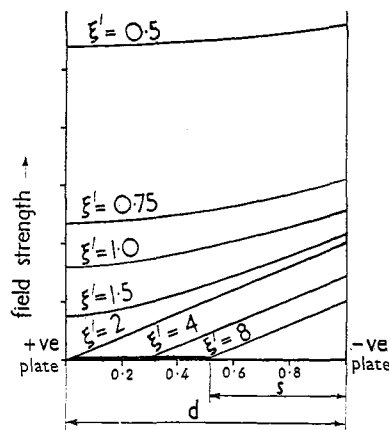


Fig. 4. Variation of field strength across the air gap when the electrons cross the gap without attachment, for several different values of ξ'

From the field distribution given by equation (22) one can calculate the positive and negative charge densities present at any plane x . The rate of recombination at x is then given by $(\alpha/e)\rho_1\rho_2$. By integrating this expression over the whole width of the gap one obtains the total recombination occurring per unit time, and hence the collection efficiency. The algebra involved in this integration is tedious and on substituting the appropriate numerical values into the final result, one finds that, as long as X_0 differs even very slightly from zero, the proportion of ions and electrons which recombine, is negligible. Until recently the recombination coefficient for electrons and positive ions in argon was thought to be about 2×10^{-10} cm³/sec, but measurements by Biondi and Brown⁽¹⁸⁾ using microwave techniques have given the much higher value of 3×10^{-7} cm³/sec. This is the value which was used in the numerical test just described. What then is the field distribution for collection efficiencies lower than unity when electrons are the negative charge carriers?

As the applied voltage V is decreased, the field X_0 at the positive plate falls until, at a certain voltage V' , we have $X_0 \simeq 0$. The field strength between the plates then follows the simple law [cf. equation (21)]

$$X = \sqrt{\left(\frac{\theta}{2} \right)} x = \sqrt{\left[\frac{4\pi q(k_1 + k_2)}{k_1 k_2} \right]} x \tag{24}$$

If the applied voltage be reduced below V' , the point of (almost) zero field must shift towards the negative plate, for we see from equation (24) that dX/dx depends only on q, k_1 and $k_2,$ and so the slope of the line cannot change as V is reduced. When the applied voltage is less than V' there is, therefore, a region of width $(d - s)$ (Fig. 4), in which the field is extremely low. This is only possible, of course, if the net space charge is negligible, that is to say, if electrons and positive ions are present in nearly equal concentrations in this region. These concentrations will be in equilibrium when the rate of recombination equals the rate of production, i.e. when

$$(\alpha/e)\rho_1\rho_2 = q \text{ or } \rho_1 = \rho_2 = \sqrt{(qe/\alpha)}$$

The saturation curve at high ionization intensity

The width of the region s is obtained from the relation

$$V = \int_0^s X dx = \frac{s^2}{2} \sqrt{\left(\frac{\theta}{2}\right)}$$

Hence
$$s = \sqrt{\left(\frac{2V\sqrt{2}}{\sqrt{\theta}}\right)} = \sqrt[4]{\left[\frac{k_1 k_2 V^2}{\pi q (k_1 + k_2)}\right]} \quad (25)$$

Now in this case the collection efficiency f is simply the ratio s/d .

Hence
$$f = \frac{s}{d} = \sqrt[4]{\left[\frac{V^2}{d^4 q} \frac{k_1 k_2}{\pi (k_1 + k_2)}\right]} = \sqrt{\frac{2}{\xi'}} \quad (26)$$

For $V \gg V'$ we have $X_0 > 0$ and $f = 1$.

The foregoing approximate theory may be compared with measurements made in argon, in an ionization chamber having 0.5 mm electrode spacing [Ref. (7), Fig. 1A]. The argon was taken, without purification, from a commercial cylinder and was allowed to flow continuously through the ionization chamber. The only impurity was said to be 2% of nitrogen. Saturation curves were taken for three different ionization intensities— 10^3 , 10^4 and 10^5 e.s.u./cm³ × sec, respectively. The separate points obtained are plotted in Fig. 5 and they evidently lie on a common curve. The dashed curve (A) is that derived from equation (26), with the constants* appropriate to argon inserted in the formula, the chain-dotted curve (B) is the experimental curve for air, as given in Figs. 1 and 2, while the full line (C) is that given by equation (14) of our earlier approximate theory for ionic conduction in air, putting $m = 24.9$ in accordance with equation (15).

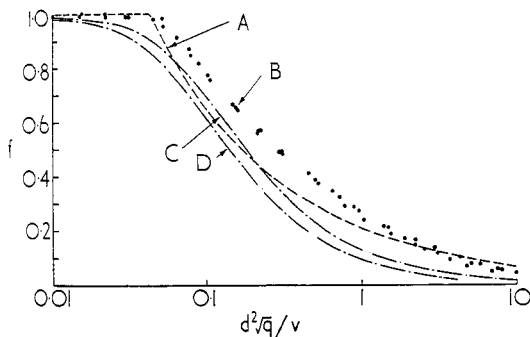


Fig. 5. General saturation curve in argon at 770 mm and 16.5°C for plane parallel geometry, at three different ionization intensities. The points were determined experimentally

A = theoretical curve for electron conduction in argon.
 B = experimental points for argon at 10^3 , 10^4 and 10^5 e.s.u./c.c. × sec.
 C = experimental curve for air ($m = 19.4$).
 D = curve for air from ionic mobilities ($m = 24.9$).

The agreement between theory and experiment is as good as could be expected, in view of the simplicity of our theoretical model, and the difficulty of measuring accurately the internal 1/2 mm airgaps in the ionization chamber. The latter was not specially designed for these measurements, but for general use. It would doubtless be possible to improve both theory and experiment, but the results presented in Fig. 5 do at least show: (i) that when the negative charge carriers are electrons, saturation curves taken at different ionization intensities coincide if plotted in terms of the parameter $d^2\sqrt{q}/V$; (ii) that

* Only k_1 is of importance in the formula since the ratio k_2/k_1 is about 1000 and k_2 therefore cancels with $(k_1 - k_2)$. For argon $k_1 \approx 1.7$ cm²/V × sec for freshly formed ions.

even in the complete absence of negative ion formation saturation difficulties arise only a little later than when negative ions are present. In Fig. 6 saturation curves in

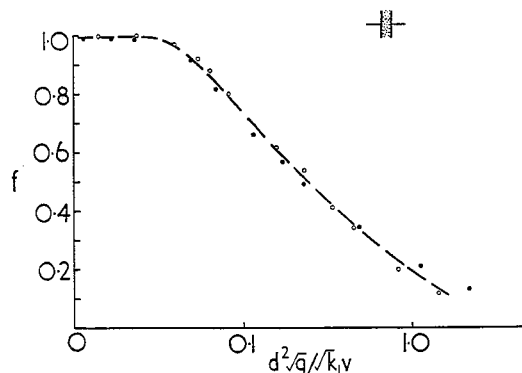


Fig. 6. General saturation curves for hydrogen and argon with plane parallel geometry, plotted in terms of the same dimensionless parameter

○ hydrogen $k_1 \approx 1.7$ cm²/V × sec } for freshly formed ions.
 ● argon $k_1 \approx 7.6$ cm²/V × sec }

hydrogen and in argon, taken under identical geometrical conditions (i.e. in the same ionization chamber) have been brought into coincidence by introducing the factor $\sqrt{k_1}$ into the denominator in order to obtain a dimensionless product in accordance with equation (3).

CYLINDRICAL AND SPHERICAL GEOMETRY

If space charge can be neglected it is not difficult to develop formulae which bring cylindrical and spherical geometry within the scope of this survey. This was done in a previous paper on pulsed radiation,⁽¹⁾ and, in the case of ionic conduction, the formulae for "equivalent gap length" are the same for continuous as for pulsed radiation. Extensive experimental investigations with variable geometry would be required to check the validity of the underlying assumptions, and these have not been made. If one considers only a particular cylindrical or spherical ionization chamber, however, saturation curves taken at different ionization intensities can be brought into coincidence by plotting f against \sqrt{q}/V .

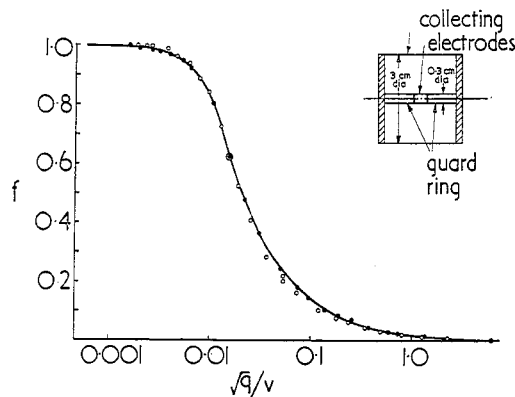


Fig. 7. Saturation curve in air at 770 mm and 16.5°C for a cylindrical ionization chamber at two different intensities

○ $q = 0.21$ e.s.u./c.c. × sec. ● $q = 0.037$ e.s.u./c.c. × sec.

In Fig. 7 two separate runs on a cylindrical chamber are plotted in this way, the intensities for the two runs differing by a factor of 6. In Fig. 8 two runs on a hemispherical chamber, differing in intensity by a factor of 4.6, are similarly plotted.

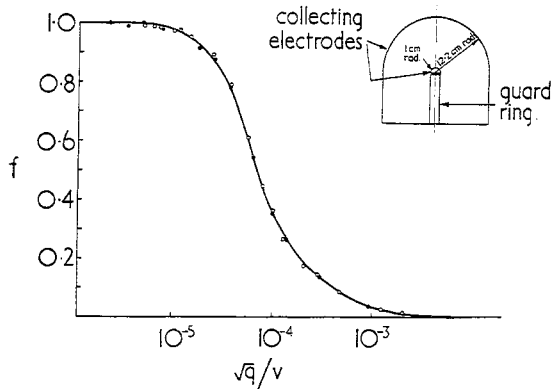


Fig. 8. Saturation curve in air at 753 mm and 16.6°C for a hemispherical ionization chamber at two different intensities

- $q = 3.4 \times 10^{-6}$ e.s.u./c.c. \times sec.
- $q = 0.73 \times 10^{-6}$ e.s.u./c.c. \times sec.

For high intensity measurements pronounced cylindrical or spherical geometry is, of course, quite unsuitable. In the first place, the radial air gap will usually have to be larger than can easily be achieved with plane electrodes, and it has to be multiplied by a factor greater than unity before it is comparable with the plane case. In the second place, the field strength at the inner electrode, due to a given applied voltage, may be several times as high as that which the same voltage would produce across a plane gap of equal length. Multiplication of ions by collision will therefore occur at considerably lower applied voltage, and this will set an upper limit to the intensity for which the ionization chamber can be used.

A spherical or cylindrical design of chamber in which the ratio of inner electrode radius to outer electrode radius approximates to unity is, on the other hand, merely a plane gap folded into a convenient form, and, provided no pockets of low field strength are permitted in the design and the gap is kept short, such a chamber is entirely suitable for high intensity work.

EMPIRICAL FORMULA FOR PRACTICAL USE

In equation (14) we have presented an empirical formula for the collection efficiency, f , in terms of the ionization intensity, q , and the other experimental variables, d and V . In practical measurements, however, q has to be estimated from the ionization current itself, and to do this one requires to know f . It is therefore worth recasting equation (14) to express f in terms of the ionization current density, i , and the other variables, d and V . We have

$$f = iqd = 2/[1 + \sqrt{1 + \frac{2}{3}\xi^2}] \tag{14}$$

where $\xi = m(d^2\sqrt{q/V})$

Hence

$$\frac{i}{qd} \frac{m^2qd^4}{6V^2} = \xi^2/3[1 + \sqrt{1 + \frac{2}{3}\xi^2}] = \eta \text{ (say)} \tag{27}$$

where $\eta = (m^2/6)(id^3/V^2)$ is a dimensionless variable embodying the current density i . If we eliminate ξ between the two equations (14) and (27) we are left with

$$f = 1/(1 + \eta) \tag{28}$$

Putting $m = 19.4$ in accordance with the experimental measurements in air, Figs. 1 and 2, we have

$$\eta = 62.7(id^3/V^2) \tag{29}$$

with i expressed in e.s.u./cm² \times sec, d in cm, and V in volts,

$$\text{or } \eta = 1.88 \times 10^5(i'd^3/V^2) \tag{30}$$

with i' in $\mu\text{A}/\text{cm}^2$.

For different atmospheric conditions, or for gases other than air, equation (28) should still provide a good fit to the saturation curve, if a suitable value is chosen for m . The appropriate value is best found by taking a complete saturation curve, plotting $(1 - f)/f$ against $id^3/6V^2$, and determining the slope of the best-fitting straight line. This slope is equal to m^2 .

UPPER LIMIT FOR IONIZATION INTENSITY

The highest ionization intensity which can be measured in a parallel plate ionization chamber depends upon (i) the minimum permissible spacing of the plates and (ii) the maximum field strength that can be used.

The minimum plate spacing is determined by the quality of workmanship available, the feasibility of measuring accurately the spacing, and the risk of floating dust bridging the gap. In our experiments we have used a chamber with a $\frac{1}{2}$ mm gap over long periods without trouble.

The maximum field strength is limited principally by the risk of ionization by collision. Provided there are no sharp points or edges in the design of the chamber, it should be possible to work up to 10 kV/cm without the occurrence of ionization by collision. On one occasion the saturation curve in air was taken up to a field of 13 kV/cm without any indication of ion multiplication. A further danger which has to be considered when thin foils are used is the deformation of the foils due to the electrostatic attraction between them. A simple calculation shows that, with the type of foil used in the present work,⁽⁷⁾ the deflexion should be negligible if the foil is adequately stretched before being cemented. This was confirmed by measuring under a microscope the deflexion of typical foils at various field strengths.

Let us consider $\frac{1}{2}$ mm spacing and 10 kV/cm as practical limits, and suppose that we are content with 90% collection. This does not mean that the 10% correction depends entirely on theory. The complete general saturation curve of the ionization chamber can be plotted at lower ionization intensity and we then depend on this curve with $d^2\sqrt{q/V}$ as abscissa, to determine the degree of saturation obtaining at the higher intensity. For $f = 0.9$ we require $d^2\sqrt{q/V}$ to be less than 0.04.

Therefore
$$\sqrt{q} = \frac{0.04 \times 10^4}{0.05} = 8000$$

that is,
$$q = 64 \times 10^6 \text{ e.s.u./c.c. } \times \text{ sec}$$

If the foregoing limits for d and V/d are replaced by the less exacting values $d = 1$ mm, $V/d = 3000$ V/cm and if we put $f = 0.9$ as before, we find

$$q = 1.44 \times 10^6 \text{ e.s.u./c.c. } \times \text{ sec}$$

Thus 10^6 e.s.u./c.c. \times sec is readily measurable in a plane parallel ionization chamber, and 10^8 e.s.u./c.c. \times sec can probably be measured with some difficulty.

REFERENCES

- (1) BOAG. *Brit. J. Radiol.*, **23**, p. 601 (1950).
- (2) THOMSON. *Conduction of electricity through gases*, Vol. 1 (London: Cambridge University Press, 1928).
- (3) MIE. *Ann. Phys., Lpz.*, **13**, p. 857 (1904).
- (4) SEELIGER. *Ann. Phys., Lpz.*, **33**, p. 319 (1910).
- (5) SEEMANN. *Ann. Phys., Lpz.*, **38**, p. 781 (1912).
- (6) BRIDGMAN. *Dimensional Analysis* (Yale University Press, 1931).
- (7) BOAG, PILLING and WILSON. *Brit. J. Radiol.*, **24**, p. 341 (1951).
- (8) TOWNSEND. *Electricity in gases*, p. 72 (London: Oxford University Press, 1915).
- (9) ERIKSON. *Phil. Mag.*, **18**, p. 328 (1909).
- (10) ERIKSON. *Phil. Mag.*, **23**, p. 747 (1912).
- (11) ERIKSON. *Phys. Rev.*, **20**, p. 117 (1922).
- (12) MASSEY. *Negative ions* (London: Cambridge University Press, 1938).
- (13) HEALEY and REED. *Behaviour of slow electrons in gases* (Sydney: Amalgamated Wireless (Australasia) Ltd., 1941).
- (14) TOWNSEND and TIZARD. *Proc. Roy. Soc. A.*, **88**, p. 336 (1913).
- (15) BAILEY. *Phil. Mag.*, **50**, p. 825 (1925).
- (16) LOEB. *Phys. Rev.*, **17**, p. 89 (1921).
- (17) LOEB. *Phil. Mag.*, **43**, p. 229 (1922).
- (18) BIONDI and BROWN. *Phys. Rev.*, **76**, p. 1697 (1949).

A method of studying the formation of cracks in a material subjected to stress

By R. JONES, B.Sc., Ph.D., Road Research Laboratory, Harmondsworth, Middlesex

[Paper received 5 November, 1951]

A method is described to determine the onset of cracking in specimens of concrete subjected to tension or compression in mechanical testing machines. While the loads were being applied, measurements were made at intervals of the velocities of ultrasonic pulses passing through the test-piece in the axial and/or transverse directions. In compression, the velocity of the ultrasonic pulses in the direction of loading remained constant while the load was increased to failure, but in the transverse direction a fall in the velocity started at only a fraction of the ultimate load, and the velocity then decreased with increase of load. This indicated that cracking occurred internally parallel to the direction of loading. The load at which it started depended on the strength of the concrete and the uniformity of the stress distribution. In tension, fracture was preceded by only a very small, and often insignificant, amount of cracking which occurred at right angles to the direction of loading.

INTRODUCTION

In recent years, considerable theoretical and experimental effort has been directed to determining the behaviour of a specimen of material loaded to failure in a mechanical testing machine. Usually, the distribution of stress across the principal cross-section is not uniform, and it is difficult to determine precisely which mechanical property of the material is being determined by the test. In some cases studies have been possible by photoelastic methods. With metallic specimens, the behaviour of the internal structure of the material when subjected to stress has been studied by X-ray crystallographic analysis. The present paper describes a method of determining the onset of cracking in specimens subjected to tension or compression, and of obtaining information concerning the orientation of such cracks. The experimental investigation has dealt solely with concrete, but this technique has been applied to examine the distribution of voids in other materials showing brittle fracture.

In the experiments to be described, cubes, cylinders, bobbins and beams of concrete were tested to destruction in mechanical testing machines of conventional design. While the loads were being applied, measurements were made at intervals of the velocities of ultrasonic pulses passing through the test-piece in the axial and/or transverse directions. The onset of cracking was indicated by a marked drop in the velocity of the pulse. In compression tests, the effects of varying the shape of the specimen, the rate of loading, and the end restraint, on the stress just causing cracking were investigated.

EXPERIMENTAL PROCEDURE

The arrangements of the test specimen and of the transducers for transmitting and receiving the ultrasonic pulses are shown diagrammatically in Fig. 1.

The velocity of the ultrasonic longitudinal waves in a given direction through the specimen was determined by accurately timing the passage of the pulse between two transducers placed in contact with opposite faces of the specimen. Both transducers contained piezoelectric quartz crystals, and each transducer had a thin film of lubricating oil between it and the concrete to improve the acoustical matching. The ultrasonic pulse was produced by electrically shock-exciting one of the transducers and, after passing through the concrete, the mechanical pulse was received by the second transducer and converted into an electrical signal. The received signal was then amplified and applied to the Y-plates of one beam of a double-beam cathode-ray tube, giving a visual trace.

Timing marks were produced on the trace of the second beam of the tube at intervals of $1.017 \mu\text{sec}$ while, to facilitate measurement, larger marks were produced at intervals of $10.17 \mu\text{sec}$. These timing marks gave the scale for determining the time taken for the leading edge of the pulse of longitudinal waves to pass through the concrete. The time of transmission was the difference between the times of arrival of the leading edge of the pulse when the transducers were placed on opposite sides of the concrete and in direct contact. A typical display on the cathode-ray tube is reproduced in Fig. 2.

The time of transmission of the pulse through the specimen in a given direction was determined before applying a load. The leading edge of the pulse on the cathode-ray tube was aligned on a cursor and also on a timing mark. When application of the load caused a change in velocity of the pulse, the change in time of arrival of the leading edge of the pulse was measured to within $0.2 \mu\text{sec}$. Full details of the apparatus have been given by Jones.⁽¹⁾

When measurements were made across the cylindrical cross-